nanomaterials

MDPI

Article

Evaluation of the Rheological Behavior and the Development of Performance Equations of Asphalt Composites Produced with Titanium Dioxide and Zinc Oxide Nanoparticles

João Victor Staub de Melo *, Alexandre Luiz Manfro, Breno Salgado Barra, Natália Dell'Antonio Cadorin and Wellington Borba Broering

Department of Civil Engineering, Federal University of Santa Catarina, Rua João Pio Duarte Silva, Florianópolis 88040-970, SC, Brazil
* Correspondence: joao.victor@ufsc.br

Abstract: This research evaluated the rheological behavior of conventional asphalt binders modified with TiO_2 and ZnO nanoparticles and proposed mathematical equations for performance prediction. First, composites were evaluated at high temperatures to investigate the Performance Grade (PG), non-recoverable creep compliance, and Aging Index (AI). Subsequently, the fatigue damage tolerance was determined at a temperature of 20 °C through the Linear Amplitude Sweep (LAS) test. At high temperatures, for both nanoparticles, stiffness gain was observed as the nanomaterial content increased, evidenced by the increase in the dynamic shear modulus. This resulted in an increase in the Performance Grade and reduction in non-recoverable creep compliance, leading to greater resistance to permanent deformations. Furthermore, it was found that nanoparticles were able to reduce the effects of oxidation of the asphalt matrix, corroborated by the reduction of the Aging Index (AI). Regarding the fatigue damage tolerance, for both nanoparticles, an increase in performance was observed at low deformation amplitudes and a decrease at high deformation amplitudes. Finally, the analysis of each rheological parameter allowed to define the mathematical equations capable of predicting the performance of conventional asphalt binders when modified with nano-TiO_2 or nano-ZnO.

Keywords: nanoparticles; titanium dioxide; zinc oxide; asphalt composites; rheological behavior; performance model; mathematical equations

check for updates

Citation: Staub de Melo, J.V.; Manfro, A.L.; Barra, B.S.; Dell'Antonio Cadorin, N.; Borba Broering, W. Evaluation of the Rheological Behavior and the Development of Performance Equations of Asphalt Composites Produced with Titanium Dioxide and Zinc Oxide Nanoparticles. *Nanomaterials* **2023**, *13*, 288. https://doi.org/10.3390/nano13020288

Academic Editor: Henrich Frielinghaus

Received: 30 December 2022
Revised: 5 January 2023
Accepted: 8 January 2023
Published: 10 January 2023

Copyright: © 2023 by the authors. Licensee MDPI, Basel, Switzerland. This article is an open access article distributed under the terms and conditions of the Creative Commons Attribution (CC BY) license (https://creativecommons.org/licenses/by/4.0/).

1. Introduction

In the last decade, researchers began to study the incorporation of nanometric semiconductors in asphalt mixtures [1–8]. In this context, TiO_2 and ZnO nanoparticles are among the most investigated semiconductors due to their low toxicity, high chemical stability, and adequate potential for oxidation processes [5].

One of the main methods for adding nanometric semiconductors to asphalt concrete consists of mixing nanoparticles with the asphalt binder [8]. In this process, the asphalt binder is heated until the desired viscosity is reached so that nanoparticles can be properly dispersed [9–11].

However, one must avoid that the properties of conventional materials are damaged due to modification. Thus, when adding new functionalities to the asphalt matrix, one must necessarily avoid compromising its mechanical performance, as it is necessary to investigate the mechanical and rheological parameters related to the developed composite [12].

The literature reports the impacts of adding TiO_2 and ZnO nanoparticles to asphalt binders: nano-TiO_2 decreases the penetration grade and increases the softening point of binders [13], increases toughness [14], increases the rutting resistance [15], increases stiffness [4], and improves resistance to aging of asphalt binders [16]; nano-ZnO increases the softening point and the binder viscosity [17], decreases the penetration grade [3],

increases the anti-aging ability [18,19], improves the shear resistance [20], and the dispersion of copolymer SBS in the asphalt [21] and decreases the acidity of the asphalt binder [22].

Despite the existence of studies addressing the use of nanometric semiconductors as modifiers of asphalt matrices [9,23–25], there is still a lack of studies that comparatively analyze the mechanical/rheological performance of composites produced with nano-TiO_2 and nano-ZnO. In this way, the definition of mathematical equations for predicting the performance of these composites can contribute to the area of knowledge, allowing the comparison between asphalt binders modified by TiO_2 and ZnO nanoparticles.

Therefore, the present study evaluates the rheological behavior of asphaltic composites in order to propose mathematical equations for performance prediction. For this purpose, asphalt composites were produced from a conventional asphalt binder modified with nano-TiO_2 and nano-ZnO, being evaluated for their mechanical performance in terms of susceptibility to permanent deformation and fatigue damage tolerance.

2. Materials and Methods

2.1. Materials

To carry out this study, the following materials were used: conventional asphalt binder obtained from "Presidente Getúlio Vargas" Refinery (REPAR/Petrobras, Araucária - PR, Brazil), zinc oxide (nano-ZnO), and titanium dioxide (nano-TiO_2) (Nanostructured & Amorphous Material, Inc., Houston, TX, USA). Table 1 presents the asphalt binder properties.

Table 1. Asphalt binder properties.

Properties	Results
High Temperature Performance Grade [26]	PG 58-XX
Penetration [27]	60×10^{-1} mm
Softening point [28]	49.5 °C
Apparent viscosity at 135 °C (20 rpm) [29]	0.326 Pa·s
Apparent viscosity at 150 °C (50 rpm) [29]	0.178 Pa·s
Apparent viscosity at 177 °C (100 rpm) [29]	0.064 Pa·s
Flash point [30]	280 °C
Relative density at 20 °C [31]	1.012
Penetration Index (Pfeiffer e Van Doormaal) [32]	−0.9

Nanoparticles were obtained from Nanostructured & Amorphous Material, Inc. (Houston, USA) and have the following characteristics:

- nano-TiO_2: predominantly consisting of titanium and oxygen, also containing copper $\leq$ 3 ppmv, cadmium $\leq$ 8 ppmv, manganese $\leq$ 5 ppmv, lead $\leq$ 9 ppmv and arsenic $\leq$ 5 ppmv (Energy-Dispersive X-ray Spectroscopy); purity of 99%; ellipsoidal and spherical shape (Figure 1A); average size of individual particles of 29.3 $\pm$ 10.6 nm; specific surface area of 60 m^2/g; density of 3.9 (20 °C); and pH between 5.5 and 5.7.
- nano-ZnO: predominantly consisting of zinc and oxygen, also containing copper $\leq$ 3 ppmv; cadmium $\leq$ 8 ppmv; manganese $\leq$ 5 ppmv; lead $\leq$ 9 ppmv and arsenic $\leq$ 5 ppmv (Energy-Dispersive X-ray Spectroscopy); purity of 99%; spherical shape (Figure 1B); average size of individual particles of 31.3 $\pm$ 8.7 nm; specific surface area of 40 m^2/g; density of 5.6 (20 °C); and pH between 6.5 and 7.5.

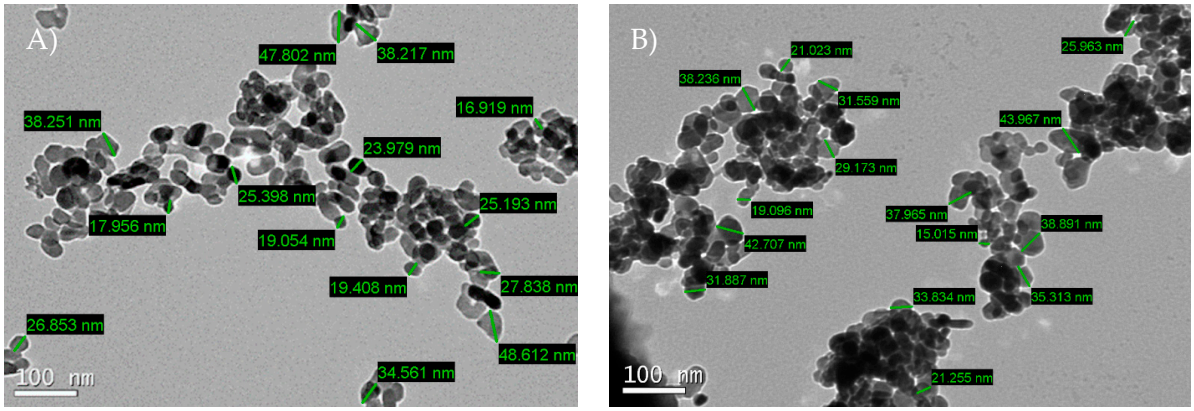


Figure 1. Nano-TiO_2 (**A**) and nano-ZnO (**B**) micrographs obtained by transmission electron microscopy technique.

Nanoparticles were also characterized in terms of crystalline structure using the X-ray diffraction technique. According to diffractograms (Figure 2), 11 well-defined peaks are verified for both materials, indicating that TiO_2 presents a tetragonal crystalline system (anatase) (according to the JCPDS 21-1272 catalog card [33–37]) and nano-ZnO presents a hexagonal crystalline system (wurtzite) (according to the JCPDS 79-2205 catalog card [38,39]).

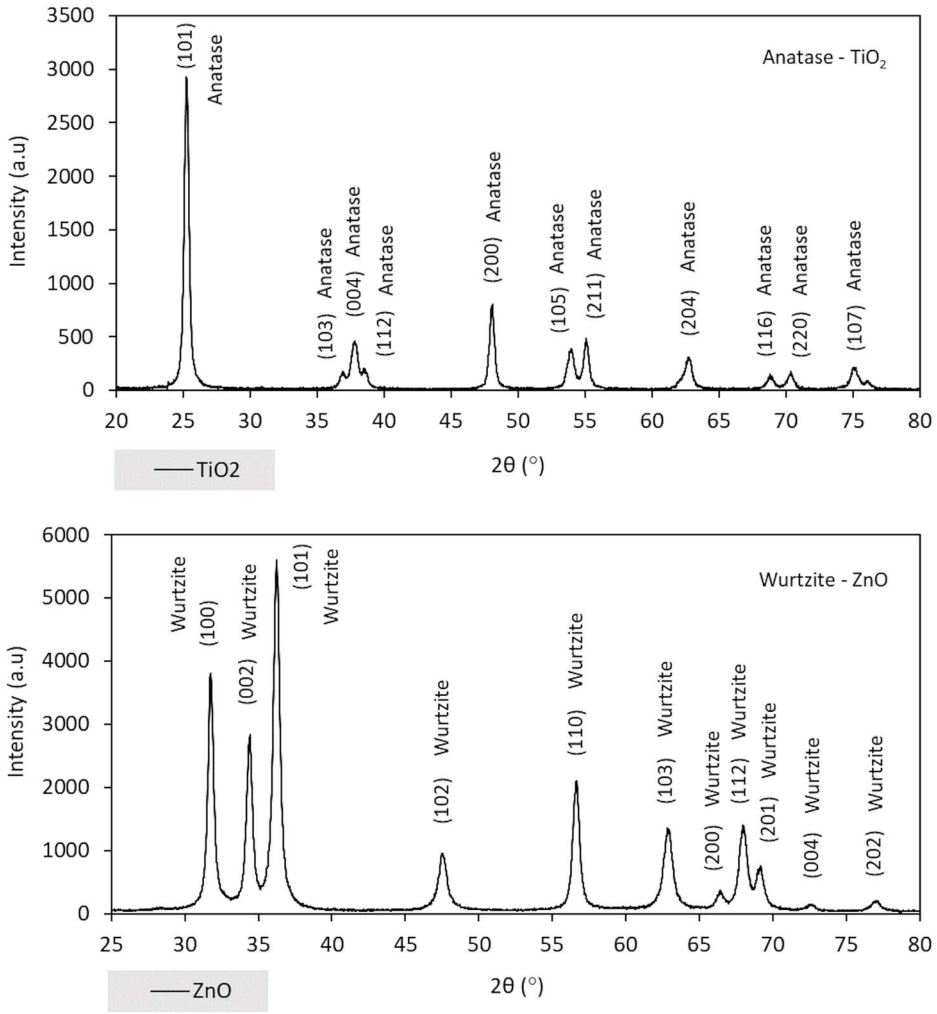


Figure 2. X-ray diffractograms: nano-TiO_2 and nano-ZnO.

In addition to primary materials, five asphalt composites with the incorporation of nano-TiO_2 (3%, 6%, 9%, 12% and 15%) and five with the incorporation of nano-ZnO (3%, 6%, 9%, 12% and 15%), in relation to the binder mass, were produced for this study. Nanomodification was carried out with an amount of binder of 300 mL at temperature of 150 ± 5 °C (apparent viscosity of 0.178 Pa.s), with high-shear mixer at a speed of 6000 rpm for 15 min. The modification temperature was defined as a function of the base binder viscosity, taking as reference the viscosity range used for the production of asphalt mixtures (0.150 to 0.190 Pa.s) [40]. The validation of the nanomodification temperature was performed through the thermogravimetry test shown in Figure 3, where the thermal stability of nanoparticles at the defined temperature was verified. According to Figure 3, the results showed that at 150 °C, there is mass loss of 5.44% (94.56%) and 1.18% (98.82%) for nano-TiO_2 and nano-ZnO, respectively, caused only by the loss of structural and adsorbed water (sample dehydration), and that the degradation of materials occurs at temperatures above 500 °C.

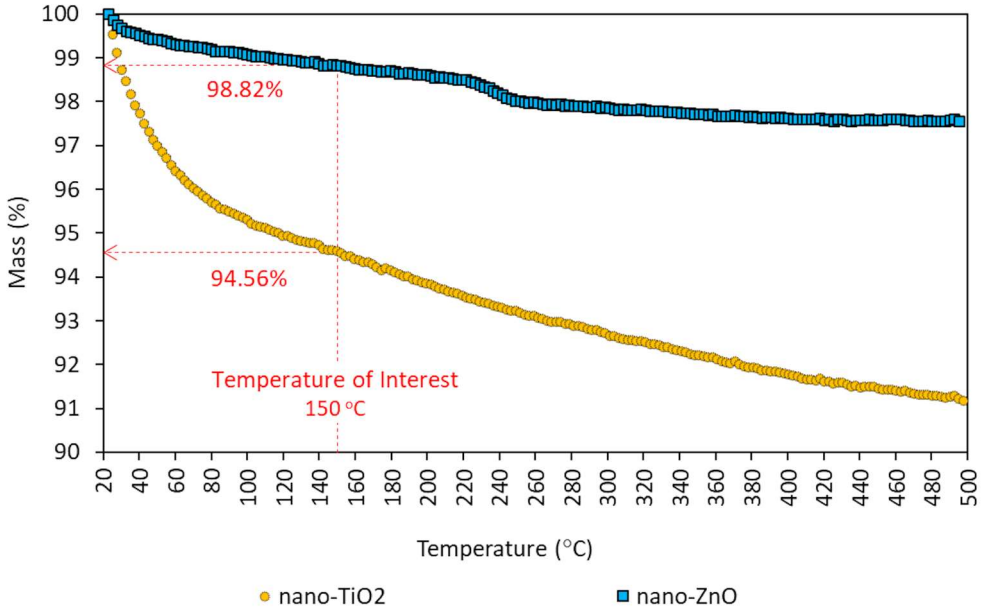


Figure 3. Thermogravimetric curve in nitrogen atmosphere: nano-TiO_2 and nano-ZnO.

2.2. Methods

To achieve the main aim of this research, the following methodological steps were established: (i) evaluation of the influence of nanoparticles on rheological parameters indicative of resistance to permanent deformation of the asphalt matrix; and (ii) performance of composites in terms of fatigue damage tolerance.

2.2.1. Evaluation of the Influence of Nanoparticles on Rheological Parameters Indicative of Resistance to Permanent Deformation of the Asphalt Matrix

The effects of incorporating nanoparticles on the rheological parameters of the asphalt binder related to permanent deformation were evaluated using a dynamic shear rheometer (HR-2, TA Instruments, Discovery Hybrid Rheometer, New Castle, USA). For this, asphalt binder samples nanomodified with nano-TiO_2 and nano-ZnO, as well as conventional binder (reference), were tested at high temperatures (58 °C, 64 °C, 70 °C, 76 °C and 82 °C). In this temperature range, the dynamic shear modulus (|G*|) and phase angle (delta—δ) were investigated in short-term aged samples (Rolling Thin-Film Oven Test—RTFOT [41]). Tests were conducted at a frequency of 10 rad/s (1.59 Hz), under controlled deformation of 10%, according to requirements of ASTM D6373 [26], ASTM D7643 [42], and ASTM D7175 standards [43]. Additionally, the performance of aged matrices (RTFOT [41]) was verified in the Multiple Stress Creep and Recovery (MSCR) test, according to ASTM D7405 [44], at

temperatures of 58 °C and 64 °C; this temperature range is used to evaluate the resistance to permanent deformation of asphalt mixtures [45–47]. The parameters evaluated in this test were the recovery rate ($\%R_{3.2}$) and the non-recoverable creep compliance ($Jnr_{3.2}$) at a stress of 3.2 kPa. For all tests carried out at high temperatures in the rheometer, samples with a geometry of 25 mm in diameter and gap of 1 mm in height were used in duplicates. In addition to this test, the effect of nanoparticles on the binder Aging Index (AI) was determined, obtained by the ratio between the rheological parameter $|G^*|/\sin \delta$ after and before (virgin condition) short-term aging in RTFOT.

Finally, based on laboratory results, equations were obtained to predict the behavior of the conventional binder as a function of the percentage of nanoparticle incorporation (TiO_2 and ZnO) to the matrix. The following equations were developed:

- An equation for TiO_2 and another for ZnO for predicting parameter $|G^*|/\sin \delta$ of the conventional aged binder (RTFOT) as a function of temperature and percentage of nano incorporation. The equations allow the classifying of the conventional binder with TiO_2 or ZnO nanoparticles in relation to the High Temperature Performance Grade (PGH).
- An equation for TiO_2 and another for ZnO for predicting the non-recoverable creep compliance ($Jnr_{3,2}$) of the conventional aged binder (RTFOT) as a function of temperature and percentage of nano incorporation. The equations allow the classifying of the conventional binder with TiO_2 or ZnO nanoparticles in relation to the traffic level, proposed by AASHTO M 332 [48].
- An equation for TiO_2 and another for ZnO for predicting the influence of nanoparticles on the conventional binder Aging Index (AI) as a function of temperature and percentage of nano incorporation.

It should be noted that the equations are suitable for any asphalt matrix that has the following initial characteristics: penetration between 50 and 70 tenths of millimeter and/or PG 58-XX.

2.2.2. Performance of Composites Regarding Fatigue Damage Tolerance

The effect of the asphalt binder modified with nano-TiO_2 and nano-ZnO on the fatigue damage tolerance was determined using the Linear Amplitude Sweep (LAS) test (AASHTO TP 101 [49]) in aged residues (RTFOT [41]). Tests were conducted using the Discovery Hybrid Rheometer (HR-2, TA Instruments, New Castle, USA) at temperature of 20 °C, frequency of 10 Hz, and strain range from 0% to 30% (3100 loading cycles). The rupture criterion was defined as a 35% reduction in the $|G^*| \cdot \sin \delta$ value of the intact material, as recommended by Chen, Zhang, and Bahia [50] and Chen and Bahia [51], thus obtaining the fatigue law ($Nf = A(\gamma_{max})^B$) of asphalt matrices (reference and nanomodified). Samples were tested in duplicate, with a geometry of 8 mm in diameter and gap of 2 mm in height.

Finally, based on results, an equation for TiO_2 and another for ZnO was obtained to predict the number of cycles to fatigue failure (Nf) of the conventional aged binder (RTFOT) as a function of the percentage of nano incorporation and deformation amplitude (γ_{max}) (at temperature of 20 °C and frequency of 10 Hz). The equations allow for the verification of the behavior of the matrix in terms of damage tolerance for any asphalt matrix with the following initial characteristics: penetration between 50 and 70 tenths of millimeter and/or PG 58-XX.

3. Results and Discussion

3.1. Evaluation of the Influence of Nanoparticles on Rheological Parameters Indicative of Resistance to Permanent Deformation of the Asphalt Matrix

Figures 4 and 5 present, respectively, the phase angle and dynamic shear modulus results of nanomodified and reference asphalt matrices. Values are characteristic of short-term aged residues, investigated at high temperatures, between 58 °C and 82 °C.

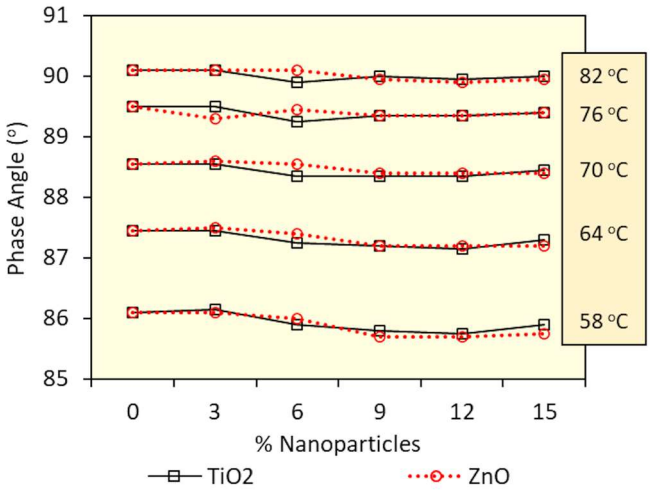


Figure 4. Comparison of the effect of the percentage of TiO_2 and ZnO on the phase angle (δ) of the conventional binder short-term aged at high temperatures (58 °C to 82 °C).

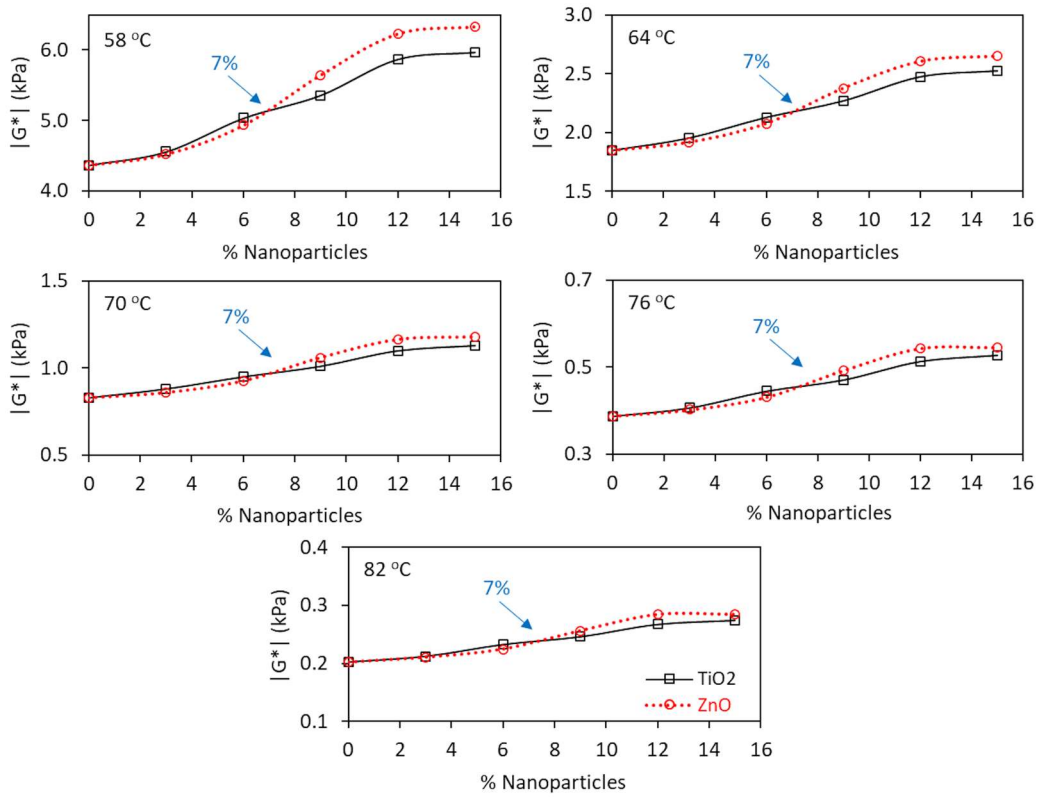


Figure 5. Comparison of the effect of the percentage of TiO_2 and ZnO on the dynamic shear modulus (|G*|) of conventional binder short-term aged at high temperatures (58 °C to 82 °C).

Based on the results presented in Figure 4, it is possible to verify that none of the nanoparticles under study (TiO_2 or ZnO) in the incorporation range of up to 15% provided significant changes in the phase angle of the original matrix. In addition, at all evaluated temperatures (58 °C to 82 °C), no tendency to increase or decrease was observed when nanoparticles were added, as well as no difference in behavior was observed regarding the type of nanoparticle used. These results allow us to conclude that nanoparticles, when added up to 15%, do not impact the elastic response of the matrix at high temperatures.

Regarding the dynamic shear modulus, it was observed in Figure 5 that the addition of nanoparticles increases the matrix stiffness at all temperatures; however, with greater impact at 58 °C and 64 °C.

The incorporation of nano-TiO_2 or nano-ZnO in the asphalt matrix results in increase in the modulus due to the nature of nanoparticles, which are not viscous but crystalline, with a small dimension and high specific surface area, which facilitates the matrix reinforcement, increasing its consistency and, consequently, its stiffness. The phase angle does not change because nanoparticles cannot add elasticity to the matrix, since they are not elastic particles but crystalline solids. However, these nanoparticles in polymeric/rubber asphalt binders, in certain percentages, can amplify the elastic capacity of the matrix [52].

Finally, with regard to the comparison between TiO_2 and ZnO, two behavior phases stand out: one with incorporations smaller than 7%, where nanoparticles present similar performance, and another, with additions greater than 7%, where ZnO makes the matrix stiffer when compared to TiO_2. The beginning of a plateau from 12% incorporation is also observed, with peak at 15%, regardless of type of nanoparticle. The performance peak represents the maximum values of rheological parameter $|G^*|/\sin \delta$, indicative of the contribution of the binder to permanent deformation, guaranteeing these composites (with 15% TiO_2 and 15% ZnO) less susceptibility to permanent deformation when compared to the other matrices. In this context, Figure 6 shows the impact of TiO_2 and ZnO incorporations in the peak region (15% of nanoparticles) in terms of $|G^*|$ and δ.

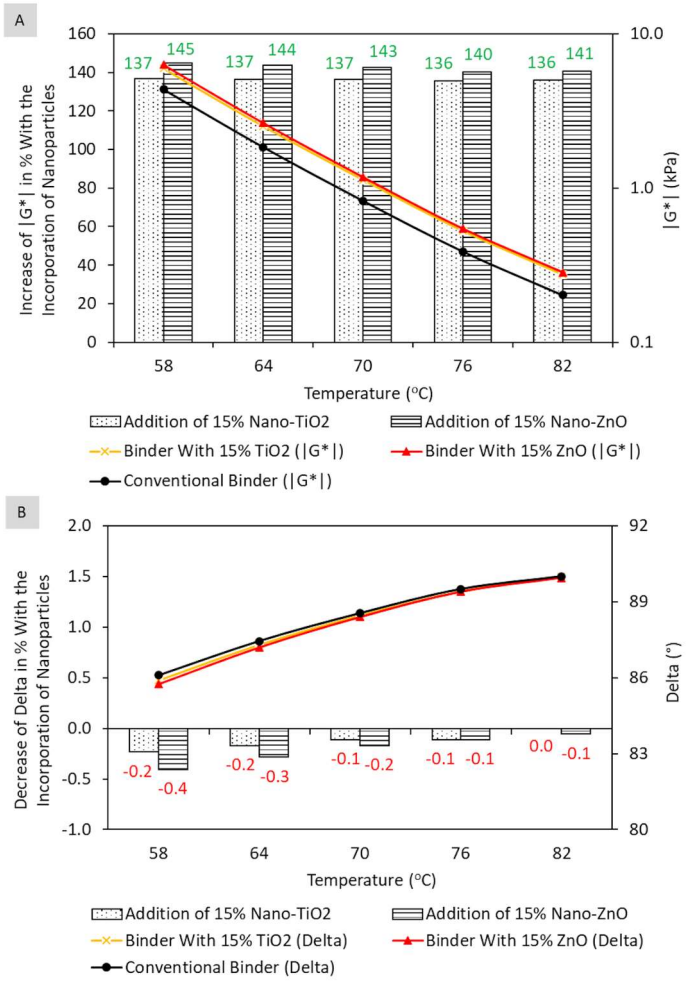


Figure 6. Influence of the incorporation of 15% of nanoparticles on the dynamic shear modulus ($|G^*|$) (**A**) and phase angle (δ) (**B**) of the asphalt matrix aged in the short term at high temperatures.

As shown in Figure 6A, the incorporation of 15% of nanoparticles in the asphalt binder, considering all temperatures, causes an average increase in the dynamic shear modulus of 136.3 ± 0.4% when using nano-TiO_2 and 142.4 ± 1.9% when using nano-ZnO. Regarding the phase angle, it is possible to verify (Figure 6B) average delta reduction of 0.13 ± 0.09% with nano-TiO_2 and 0.21 ± 0.14% with nano-ZnO, considering all temperatures. Thus, as the change in the phase angle with nanomodification is negligible, the parameter $|G^*|/\sin\delta$ increases practically in the same proportion as the dynamic shear modulus, that is, by 136.3 ± 0.5% and 142.6 ± 2.0%, when incorporating 15% nano-TiO_2 and 15% nano-ZnO, respectively.

Mathematical equations used to predict the parameter $|G^*|/\sin\delta$ of the aged binder (RTFOT) as a function of temperature and the percentage of nano incorporation are presented by Equations (1) and (2). These equations allow to predict the classification of any conventional binder (PG 58-XX) in relation to the High Temperature Performance Grade (PGH) when TiO_2 or ZnO nanoparticles are incorporated.

$$\frac{|G*|}{\sin\delta}\{\%TiO_2,\ T\} = \frac{\left(77.14 \times 10^{13} \times \%TiO_2\right) + \left(23.82 \times 10^{15}\right)}{T^{(0.0014 \times \%TiO_2) + 8.9219}} \quad (1)$$

$$\frac{|G*|}{\sin\delta}\{\%ZnO,\ T\} = \frac{\left(18.56 \times 10^{14} \times \%ZnO\right) + \left(23.82 \times 10^{15}\right)}{T^{(0.0066 \times \%ZnO) + 8.9219}} \quad (2)$$

where: $|G^*|/\sin\delta$ = is the rheological parameter (kPa) T = is the temperature (°C).

Additionally, Figure 7 presents the results regarding the Multiple Stress Creep and Recovery (MSCR) test at stress of 3.2 kPa (average of 10 cycles), performed immediately after 20 cycles of creep and recovery at stress of 0.1 kPa. Each value is characteristic of the average of two short-term aged samples.

According to Figure 7, it is possible to verify for both investigated temperatures (58 °C and 64 °C) that the conventional binder presents the worst behavior in relation to the non-recoverable creep compliance ($Jnr_{3.2}$). At a temperature of 58 °C, $Jnr_{3.2}$ was 2.23 kPa^{-1} for the conventional binder, 1.66 kPa^{-1} for binder with nano-TiO_2 (15%), and 1.42 kPa^{-1} for binder with nano-ZnO (15%). As the temperature increased to 64 °C, $Jnr_{3.2}$ increased for all matrices, resulting from the thermal susceptibility of the asphalt. However, the performance hierarchy remained, where $Jnr_{3.2}$ was 5.45 kPa^{-1} for the conventional binder, 4.03 kPa^{-1} for binder with nano-TiO_2 (15%), and 3.84 kPa^{-1} for binder with nano-ZnO (15%). Considering both temperatures, the addition of nanoparticles caused an average reduction of the parameter in relation to the conventional binder of 25.8 ± 0.3% when adding nano-TiO^2 and 33.0 ± 4.7% when adding nano-ZnO. As for the recovery rate ($\%R_{3.2}$), all matrices showed values below 2%, characterizing low elasticity, confirming that these nanoparticles are not able to provide elasticity to the matrix.

The better performance of composites in the test is due to the greater stiffness of these matrices as a result of the nanometric reinforcement. This finding is confirmed by analyzing the final strain value (ε_1) of binders after applying a stress of 3.2 kPa (constant) for 1 s. Considering the 10 loading cycles (3.2 kPa), the mean values for each matrix were the following: (a) at 58 °C: ε_1 = 7.20 ± 0.05% (conventional binder); ε_1 = 5.38 ± 0.05% (composite with TiO_2); ε_1 = 4.61 ± 0.06% (composite with ZnO); (b) at 64 °C: ε_1 = 17.41 ± 0.13% (conventional binder); ε_1 = 12.91 ± 0.14% (composite with TiO_2); and ε_1 = 12.29 ± 0.25% (composite with ZnO). In summary, considering both temperatures, matrices nanomodified with TiO_2 and ZnO present deformation 25.6 ± 0.4% and 32.7 ± 3.4% less than the conventional matrix. Thus, the results obtained in the MSCR test corroborate the behavior observed in matrices regarding the dynamic shear modulus ($|G^*|$) and phase angle (delta—δ). It could be concluded that composites are less susceptible to permanent deformation than the conventional binder. The performance gain of composites is related to the nature of nanoparticles, and both are small in size, have high specific

surface area, crystalline, with high mechanical strength and structural stability, allowing the reinforcement of the matrix nanostructure.

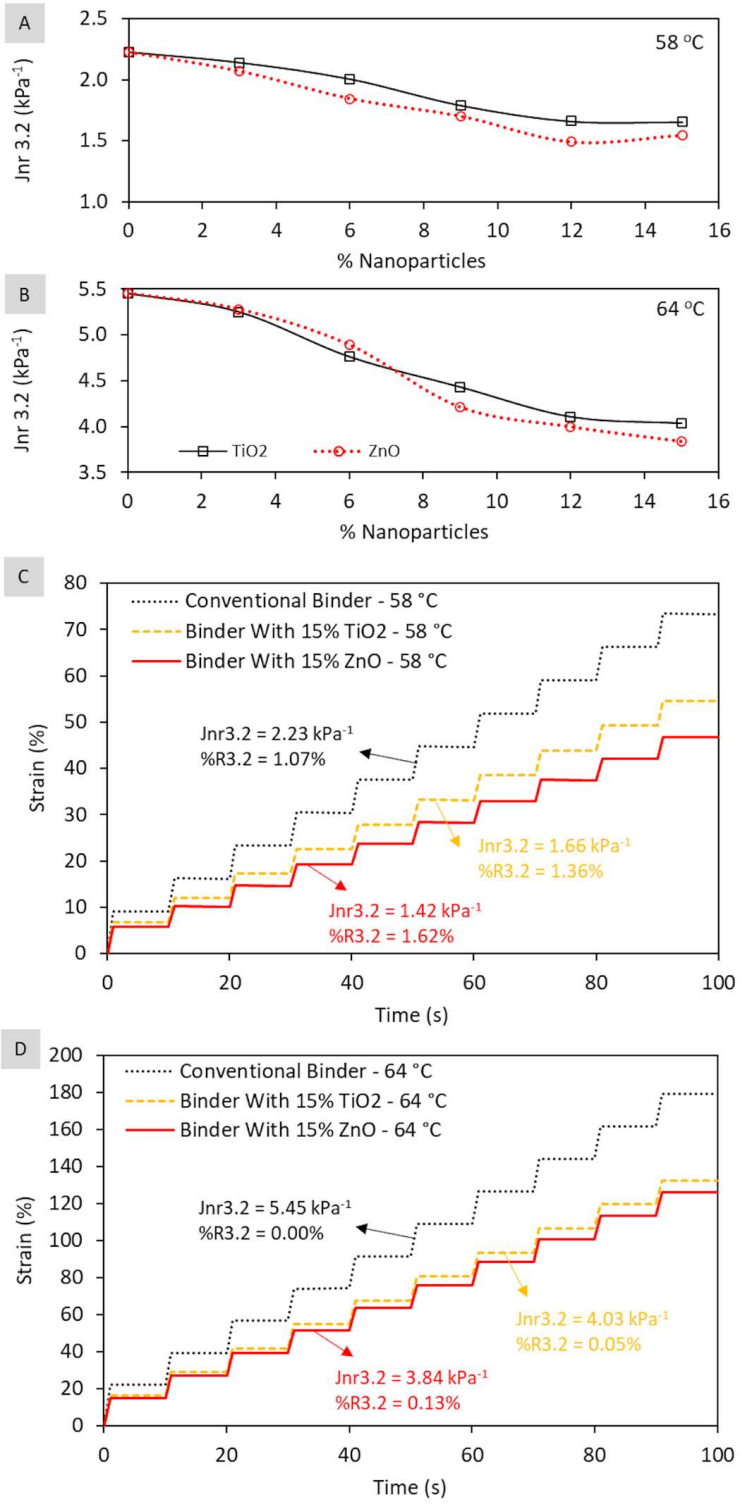


Figure 7. Behavior of asphalt matrices (after RTFOT) in terms of creep and recovery during the MSCR test at stress of 3.2 kPa: non-recoverable creep compliance as a function of the percentage of nanoparticle at temperature of 58 °C (**A**) and at temperature of 64 °C (**B**) and comparison of creep and recovery curves of the conventional binder in relation to composites with 15% TiO_2 and 15% ZnO at temperature of 58 °C (**C**) and at temperature of 64 °C (**D**).

Equations (3) and (4) show the non-recoverable creep compliance ($Jnr_{3.2}$) prediction equations of the aged binder (RTFOT) as a function of temperature and percentage of nanoparticles (TiO_2 or ZnO) added to the matrix. The equations allow to predict the classification of any conventional binder (PG 58-XX) with TiO_2 or ZnO nanoparticles in relation to the traffic level proposed by the AASHTO M 332 standard [48].

$$J_{nr3.2}\ \{\%TiO_2,\ T\} = \left[\left(-9.33\ \times\ 10^{-19}\ \times\ \%TiO_2\right) + \left(1.97\ \times\ 10^{-16}\right)\right] T^{(-0.0033\ \times\ \%TiO_2)+9.1} \quad (3)$$

$$J_{nr3.2}\ \{\%ZnO,\ T\} = \left[\left(-7.81\ \times\ 10^{-18}\ \times\ \%ZnO\right) + \left(1.97\ \times\ 10^{-16}\right)\right] T^{(0.0093\ \times\ \%ZnO)+9.1} \quad (4)$$

where: $J_{nr3.2}$ = non-recoverable creep compliance at 3.2 kPa creep stress (kPa^{-1}) and T = is the temperature (°C).

Regarding the binder Aging Index (AI) calculated based on the rheological parameter $|G^*|/\sin\delta$ in the virgin and aged state (RTFOT), considering all test temperatures (58 °C to 82 °C), a reduction in the index was observed with the addition of nanoparticles. The average index was 2.00 ± 0.10 for the conventional matrix, 1.79 ± 0.07 for composite with 15% TiO_2, and 1.67 ± 0.10 for composite with 15% ZnO. In percentage terms, the reduction in the index is 10.7 ± 0.8% and 16.6 ± 0.7% when TiO_2 and ZnO are incorporated, respectively. It could be concluded that composites are more resistant to aging. The greater resistance is a function of the special characteristics of nanoparticles: the particle size allows to fill the matrix, blocking oxidation and volatilization; the high specific surface area and surface energy promote adsorption inside the matrix, reducing the exudation of oily compounds that adhere to the surface of particles.

Equations (5) and (6) show a model for TiO_2 and another for ZnO for predicting the influence of nanoparticles on the Aging Index (AI) for any conventional binder (PG 58-XX) as a function of temperature and percentage of nano incorporation.

$$AI\ \{\%TiO_2,\ T\} = \frac{(-0.1985\ \times\ \%TiO_2) + 9.3491}{T^{(-0.0043\ \times\ \%TiO_2)+0.364}} \quad (5)$$

$$AI\ \{\%ZnO,\ T\} = \frac{(0.0255\ \times\ \%ZnO) + 9.3491}{T^{(0.0035\ \times\ \%ZnO)+0.364}} \quad (6)$$

where: AI = Aging Index; T = is the temperature (°C).

3.2. Performance of Composites Regarding Fatigue Damage Tolerance

The effect of adding the two types of nanoparticles on the matrix behavior in terms of damage tolerance was verified by the LAS test (20 °C). Figure 8 presents the results obtained in terms of the stress–strain curve, parameters A and B of the fatigue model ($Nf = A(\gamma_{max})^B$), and percentage increase or decrease in damage tolerance (Nf) as a function of the deformation amplitude and type of nanoparticle.

According to the stress–strain curve shown in Figure 8A, the addition of nanoparticles at 15% content increases the matrix stiffness at intermediate temperatures, as the slope of the curve in the elastic region is more pronounced for composites with ZnO and TiO_2, respectively. This statement is corroborated by the maximum stress peak, with higher values for ZnO (675 kPa, 18.7% higher) and TiO_2 composites (632 kPa, 11.1% higher) compared to the conventional binder (568 kPa) in the same deformation amplitude (9.11 ± 0.09%). Comparing nanoparticles, the sample with 15% zinc oxide has a maximum stress 6.8% higher than sample with 15% titanium dioxide.

As for the fatigue model (Figure 8B), it appears that the incorporation of nanoparticles increases parameter A, where binders with nano-TiO_2 and nano-ZnO showed, respectively, an average increase of 38.9% (77,485.92) and 29.3% (72,141.28) in relation to the reference (55,778.92). For parameter B, there is an increase in value (in modulus) when nanoparticles are added to the asphalt matrix. The sample with zinc oxide had a result 8.1% (|−3.02|) higher than the reference (|−2.79|), whereas the composite with titanium dioxide showed

a value 5.8% (|−2.95|) higher. Finally, it appears that the presence of both nanoparticles increases the matrix sensitivity to the level of deformation, with greater intensity for nano-ZnO.

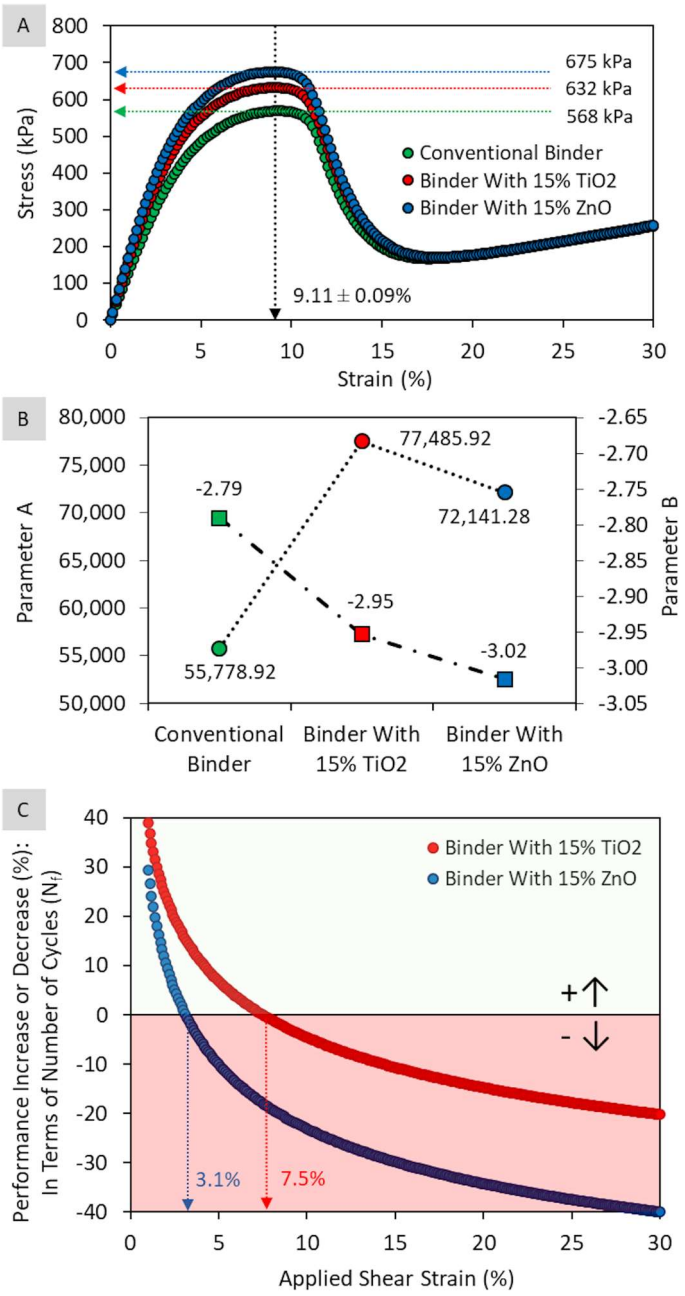


Figure 8. Results of the LAS test (20 °C): (**A**) stress-strain curve, (**B**) parameters A and B of the fatigue model, and (**C**) effect of the type of nanoparticle on the damage tolerance of the asphalt matrix (increase or decrease in performance) as a function of the deformation amplitude.

In this perspective, Figure 8C highlights the impact of incorporations on the fatigue damage tolerance as a function of the deformation amplitude. At deformation amplitudes greater than 3.1% for binder with ZnO and 7.5% for binder with TiO_2, a reduction in the number of cycles for failure (Nf) is observed when compared to the reference, where the greater the deformation amplitude, the smaller the performance of composites. Evaluating the type of nanoparticle, it was observed that the matrix modified with TiO_2 presents better fatigue damage tolerance than the matrix with ZnO, where, considering all deformation amplitudes, the number of cycles until failure is on average 25.9 ± 6.0% higher.

It could be concluded that the addition of nanoparticles in the asphalt matrix is beneficial in terms of fatigue damage tolerance at small deformation amplitudes, impairing the resulting behavior at higher deformation amplitudes. In this case, for amplitudes of 15%, pointed out by Chen, Zhang, and Bahia [50] and Chen and Bahia [51] as a region with stronger correlation with the fatigue life of asphalt mixtures, there is strong indication of a negative effect of the incorporation of these two nanoparticles. Composites would present performance loss in relation to the conventional binder in the order of 10.6% and 28.8%, when incorporating nano-TiO_2 and nano-ZnO in the asphalt matrix, respectively. However, it is emphasized that there are no studies in literature on the effective prediction of parameters obtained in the LAS test regarding nanomodified mixtures.

Equations (7) and (8) show performance prediction equations regarding fatigue for conventional asphalt binders (PG 58-XX) modified with nano-TiO_2 and nano-ZnO. The equations provide the number of cycles (Nf) as a function of the maximum deformation amplitude (γ_{max}) and nanoparticle content (%TiO_2 or %ZnO).

$$N_f\ \{\%TiO_2,\ \gamma_{max}\} = [1378.68(\%TiO_2) + 55,778.92](\gamma_{max})^{-0.0106(\%TiO_2)\ -\ 2.79} \quad (7)$$

$$N_f\ \{\%ZnO,\ \gamma_{max}\} = [1161.01(\%ZnO) + 55,778.92](\gamma_{max})^{-0.0147(\%ZnO)\ -\ 2.79} \quad (8)$$

where: N_f = number of cycles until failure; γ_{max} = Strain amplitude.

4. Conclusions

This study evaluated the rheological behavior of conventional asphalt binders modified with TiO_2 and ZnO nanoparticles and proposed mathematical equations for performance prediction. According to the results obtained, it could be concluded that:

- The increase in the nano-TiO_2 and nano-ZnO content in the asphalt matrix results in the improvement of rheological parameters related to performance at high temperatures, specifically parameter $|G^*|/\sin\delta$ and the non-recoverable creep compliance at a stress of 3.2 kPa. This indicates a potential gain in resistance to permanent deformation of the asphalt material;
- With the incorporation of nanoparticles, the porosity of the conventional asphalt binder was filled due to the reduced dimensions of nanoparticles (TiO_2 and ZnO), which increased impermeability and reduced the effects of oxidation and volatilization, reflecting in the reduction of the Aging Index values;
- In terms of fatigue resistance, when compared to the pure asphalt binder, both composites show increase in the number of cycles until failure at low deformation amplitudes (up to 7.5% for binders with nano-TiO_2 and up to 3.1% for binders with nano-ZnO). On the other hand, at high deformation amplitudes, the opposite was observed. This behavior is intensified as the nanoparticle content increases. This points to an increase in sensitivity to the deformation level;
- In the comparison between composites, the binder modified with nano-TiO_2 presents a higher number of cycles during the assessment of the fatigue damage tolerance, whereas the binder with nano-ZnO indicates better mechanical and rheological response at high temperatures; and
- It was possible to define mathematical performance equations for each rheological parameter, providing a perspective for predicting the behavior of conventional asphalt binders (PG 58-XX) when modified with nano-TiO_2 or nano-ZnO.

Author Contributions: Conceptualization, J.V.S.d.M., A.L.M., B.S.B., N.D.C. and W.B.B.; methodology, J.V.S.d.M., A.L.M., B.S.B., N.D.C. and W.B.B.; validation, J.V.S.d.M., A.L.M., B.S.B. and N.D.C.; formal analysis, J.V.S.d.M., A.L.M., B.S.B. and N.D.C.; investigation, J.V.S.d.M., A.L.M., B.S.B., N.D.C. and W.B.B.; resources, J.V.S.d.M.; data curation, J.V.S.d.M., A.L.M., B.S.B. and N.D.C.; writing—original draft preparation, J.V.S.d.M. and A.L.M.; writing—review and editing, J.V.S.d.M. and A.L.M.; visualization, J.V.S.d.M., A.L.M., B.S.B., N.D.C. and W.B.B.; supervision, J.V.S.d.M.; project administration, J.V.S.d.M.; funding acquisition, J.V.S.d.M. All authors have read and agreed to the published version of the manuscript.

Funding: This research was funded by National Council for Scientific and Technological Development—CNPq (Call MCTIC/CNPq No. 28/2018—Process: 420614/2018-4) and the Coordination for the Improvement of Higher Education-Personnel—CAPES (Financing Code 001).

Data Availability Statement: The data presented in this study are available on request from the corresponding author.

Acknowledgments: The authors would like to thank the Asphalt/Petrobras Thematic-Network for the investments made in the Laboratory of Paving at UFSC and the following laboratories: Laboratory of Paving (LabPav/ECV/UFSC), Laboratory of Nanotechnology (LabNANOTEC/ECV/UFSC), Central Laboratory of Electronic Microscopy (LCME/UFSC), and Laboratory of Control and Polymerization Processes (LCP/EQA/UFSC) and Analysis Center (EQA/UFSC).

Conflicts of Interest: The authors declare no conflict of interest. The funders had no role in the design of the study; in the collection, analyses, or interpretation of data; in the writing of the manuscript; or in the decision to publish the results.

References

1. de Rosso, L.T.; Staub de Melo, J.V. Impact of Incorporating Recycled Glass on the Photocatalytic Capacity of Paving Concrete Blocks. *Constr. Build. Mater.* **2020**, *259*, 119778. [CrossRef]
2. Trujillo-Valladolid, M.; Alcántar-Vázquez, B.; Ramírez-Zamora, R.-M.; Ossa-López, A. Influence of Aging on the Physicochemical Behavior of Photocatalytic Asphalt Cements Subjected to the Natural Environment. *Constr. Build. Mater.* **2021**, *295*, 123597. [CrossRef]
3. Xu, X.; Guo, H.; Wang, X.; Zhang, M.; Wang, Z.; Yang, B. Physical Properties and Anti-Aging Characteristics of Asphalt Modified with Nano-Zinc Oxide Powder. *Constr. Build. Mater.* **2019**, *224*, 732–742. [CrossRef]
4. Günay, T.; Ahmedzade, P. Physical and Rheological Properties of Nano-TiO2 and Nanocomposite Modified Bitumens. *Constr. Build. Mater.* **2020**, *243*, 118208. [CrossRef]
5. Bica, B.O.; de Melo, J.V.S. Concrete Blocks Nano-Modified with Zinc Oxide (ZnO) for Photocatalytic Paving: Performance Comparison with Titanium Dioxide (TiO_2). *Constr. Build. Mater.* **2020**, *252*, 119120. [CrossRef]
6. Cao, X.; Yang, X.; Li, H.; Huang, W.; Liu, X. Investigation of Ce-TiO_2 Photocatalyst and Its Application in Asphalt-Based Specimens for NO Degradation. *Constr. Build. Mater.* **2017**, *148*, 824–832. [CrossRef]
7. Hu, Z.; Xu, T.; Liu, P.; Oeser, M. Developed Photocatalytic Asphalt Mixture of Open Graded Friction Course for Degrading Vehicle Exhaust. *J. Clean. Prod.* **2021**, *279*, 123453. [CrossRef]
8. Sha, A.; Liu, Z.; Jiang, W.; Qi, L.; Hu, L.; Jiao, W.; Barbieri, D.M. Advances and Development Trends in Eco-Friendly Pavements. *J. Road Eng.* **2021**, *1*, 1–42. [CrossRef]
9. Cadorin, N.D.; de Melo, J.V.S.; Broering, W.B.; Manfro, A.L.; Barra, B.S. Asphalt Nanocomposite with Titanium Dioxide: Mechanical, Rheological and Photoactivity Performance. *Constr. Build. Mater.* **2021**, *289*, 123178. [CrossRef]
10. Ziari, H.; Amini, A.; Goli, A. The Effect of Different Aging Conditions and Strain Levels on Relationship between Fatigue Life of Asphalt Binders and Mixtures. *Constr. Build. Mater.* **2020**, *244*, 118345. [CrossRef]
11. Qian, G.; Yu, H.; Gong, X.; Zhao, L. Impact of Nano-TiO_2 on the NO_2 Degradation and Rheological Performance of Asphalt Pavement. *Constr. Build. Mater.* **2019**, *218*, 53–63. [CrossRef]
12. da Rocha Segundo, I.G.; Landi, S., Jr.; Oliveira, S.M.B.; de Freitas, E.F.; Carneiro, J.A.O. Photocatalytic Asphalt Mixtures: Mechanical Performance and Impacts of Traffic and Weathering Abrasion on Photocatalytic Efficiency. *Catal. Today* **2019**, *326*, 94–100. [CrossRef]
13. Ameli, A.; Hossein Pakshir, A.; Babagoli, R.; Norouzi, N.; Nasr, D.; Davoudinezhad, S. Experimental Investigation of the Influence of Nano TiO2 on Rheological Properties of Binders and Performance of Stone Matrix Asphalt Mixtures Containing Steel Slag Aggregate. *Constr. Build. Mater.* **2020**, *265*, 120750. [CrossRef]
14. Shafabakhsh, G.H.; Ani, O.J. Experimental Investigation of Effect of Nano TiO_2/SiO_2 Modified Bitumen on the Rutting and Fatigue Performance of Asphalt Mixtures Containing Steel Slag Aggregates. *Constr. Build. Mater.* **2015**, *98*, 692–702. [CrossRef]
15. Shafabakhsh, G.; Mirabdolazimi, S.M.; Sadeghnejad, M. Evaluation the Effect of Nano-TiO_2 on the Rutting and Fatigue Behavior of Asphalt Mixtures. *Constr. Build. Mater.* **2014**, *54*, 566–571. [CrossRef]

16. Nazari, H.; Naderi, K.; Moghadas Nejad, F. Improving Aging Resistance and Fatigue Performance of Asphalt Binders Using Inorganic Nanoparticles. *Constr. Build. Mater.* **2018**, *170*, 591–602. [CrossRef]
17. Zhang, H.; Gao, Y.; Guo, G.; Zhao, B.; Yu, J. Effects of ZnO Particle Size on Properties of Asphalt and Asphalt Mixture. *Constr. Build. Mater.* **2018**, *159*, 578–586. [CrossRef]
18. Zhang, H.; Chen, Z.; Li, L. Effect of Nanozinc Oxide and Organic Expanded Vermiculite Compound on Antiaging Properties of SBR Modified Bitumen. *J. Mater. Civ. Eng.* **2017**, *29*, 04017204. [CrossRef]
19. Duan, H.; Long, J.; Zhang, H.; Luo, H.; Cao, J. Effects of Different Carriers for Zinc Oxide (ZnO) Particles on Microstructure of ZnO/Layered Silicate Composite and Aging Resistance of Composite Modified Asphalt. *Constr. Build. Mater.* **2022**, *349*, 128773. [CrossRef]
20. Su, M.; Si, C.; Zhang, Z.; Zhang, H. Molecular Dynamics Study on Influence of Nano-ZnO/SBS on Physical Properties and Molecular Structure of Asphalt Binder. *Fuel* **2020**, *263*, 116777. [CrossRef]
21. Xie, X.; Hui, T.; Luo, Y.; Li, H.; Li, G.; Wang, Z. Research on the Properties of Low Temperature and Anti-UV of Asphalt with Nano-ZnO/Nano-TiO_2/Copolymer SBS Composite Modified in High-Altitude Areas. *Adv. Mater. Sci. Eng.* **2020**, *2020*, 1–15. [CrossRef]
22. Hamedi, G.H.; Nejad, F.M.; Oveisi, K. Estimating the Moisture Damage of Asphalt Mixture Modified with Nano Zinc Oxide. *Mater. Struct.* **2016**, *49*, 1165–1174. [CrossRef]
23. Yadykova, A.Y.; Ilyin, S.O. Rheological and Adhesive Properties of Nanocomposite Bitumen Binders Based on Hydrophilic or Hydrophobic Silica and Modified with Bio-Oil. *Constr. Build. Mater.* **2022**, *342*, 127946. [CrossRef]
24. Yadykova, A.Y.; Ilyin, S.O. Bitumen Improvement with Bio-Oil and Natural or Organomodified Montmorillonite: Structure, Rheology, and Adhesion of Composite Asphalt Binders. *Constr. Build. Mater.* **2023**, *364*, 129919. [CrossRef]
25. Rocha Segundo, I.; Ferreira, C.; Freitas, E.F.; Carneiro, J.O.; Fernandes, F.; Júnior, S.L.; Costa, M.F. Assessment of Photocatalytic, Superhydrophobic and Self-Cleaning Properties on Hot Mix Asphalts Coated with TiO_2 and/or ZnO Aqueous Solutions. *Constr. Build. Mater.* **2018**, *166*, 500–509. [CrossRef]
26. ASTM. *D6373*; Standard Specification for Performance Graded Asphalt Binder, American Association of State Highway and Transportation. ASTM: West Conshohocken, PA, USA, 2016.
27. ABNT. *NBR 6576*; Materiais Asfálticos—Determinação Da Penetração, Associação Brasileira de Normas Técnicas. ABNT: Rio de Janeiro, Brazil, 2017.
28. ABNT. *NBR 6560*; Ligantes Asfálticos—Determinação Do Ponto de Amolecimento—Método Do Anel e Bola, Associação Brasileira de Normas Técnicas. ABNT: Rio de Janeiro, Brazil, 2016.
29. ASTM. *D4402/D4402M*; Standard Test Method for Viscosity Determination of Asphalt at Elevated Temperatures Using a Rotational Viscometer, American Association of State Highway and Transportation. ASTM: West Conshohocken, PA, USA, 2015.
30. ABNT. *NBR 11341*; Derivados de Petróleo—Determinação Dos Pontos de Fulgor e de Combustão Em Vaso Aberto Cleveland, Associação Brasileira de Normas Técnicas. ABNT: Rio de Janeiro, Brazil, 2015.
31. ABNT. *NBR 6296*; Produtos Betuminosos Semissólidos—Determinação Da Massa Específica e Densidade Relativa, Associação Brasileira de Normas Técnicas. ABNT: Rio de Janeiro, Brazil, 2012.
32. Hunter, R.N.; Self, A.; Read, J. *The Shell Bitumen Handbook*, 6th ed.; ICE Publishing: Londres, UK, 2015. [CrossRef]
33. Ennaceri, H.; Boujnah, M.; Taleb, A.; Khaldoun, A.; Sáez-Araoz, R.; Ennaoui, A.; El Kenz, A.; Benyoussef, A. Thickness Effect on the Optical Properties of TiO_2-Anatase Thin Films Prepared by Ultrasonic Spray Pyrolysis: Experimental and Ab Initio Study. *Int. J. Hydrogen Energy* **2017**, *42*, 19467–19480. [CrossRef]
34. Castro-Beltrán, A.; Luque, P.A.; Garrafa-Gálvez, H.E.; Vargas-Ortiz, R.A.; Hurtado-Macías, A.; Olivas, A.; Almaral-Sánchez, J.L.; Alvarado-Beltrán, C.G. Titanium Butoxide Molar Ratio Effect in the TiO_2 Nanoparticles Size and Methylene Blue Degradation. *Optik (Stuttg)* **2018**, *157*, 890–894. [CrossRef]
35. Fernández-Arroyo, A.; Lara, M.A.; Domine, M.E.; Sayagués, M.J.; Navío, J.A.; Hidalgo, M.C. High {0 0 1} Faceted TiO_2 Nanoparticles for the Valorization of Oxygenated Compounds Present in Aqueous Biomass-Derived Feedstocks. *J. Catal.* **2018**, *358*, 266–276. [CrossRef]
36. Huang, R.; Zhang, S.; Ding, J.; Meng, Y.; Zhong, Q.; Kong, D.; Gu, C. Effect of Adsorption Properties of Phosphorus-Doped TiO2 Nanotubes on Photocatalytic NO Removal. *J. Colloid Interface Sci.* **2019**, *553*, 647–654. [CrossRef]
37. Lopes, F.C.S.M.R.; da Rocha, M.d.G.C.; Bargiela, P.; Sousa Ferreira, H.; Pires, C.A.d.M. Ag/TiO_2 Photocatalyst Immobilized onto Modified Natural Fibers for Photodegradation of Anthracene. *Chem. Eng. Sci.* **2020**, *227*, 115939. [CrossRef]
38. Erazo, A.; Mosquera, S.A.; Rodríguez-Paéz, J.E. Synthesis of ZnO Nanoparticles with Different Morphology: Study of Their Antifungal Effect on Strains of Aspergillus Niger and Botrytis Cinerea. *Mater. Chem. Phys.* **2019**, *234*, 172–184. [CrossRef]
39. Arciniegas-Grijalba, P.A.; Patiño-Portela, M.C.; Mosquera-Sánchez, L.P.; Guerra Sierra, B.E.; Muñoz-Florez, J.E.; Erazo-Castillo, L.A.; Rodríguez-Páez, J.E. ZnO-Based Nanofungicides: Synthesis, Characterization and Their Effect on the Coffee Fungi *Mycena citricolor* and *Colletotrichum* sp. *Mater. Sci. Eng. C* **2019**, *98*, 808–825. [CrossRef] [PubMed]
40. Asphalt Institute. *Asphalt Binder Testing. Superpave Series N° 2 (SP-2)*, 3rd ed.; Asphalt Institute: Lexington, KY, USA, 2001.
41. AASHTO. *AASHTO T 240*; Standard Method of Test for Effect of Heat and Air on a Moving Film of Asphalt (Rolling Thin-Film Oven Test), Test Standard Specifications for Transportation Materials and Methods of Sampling and Testing. AASHTO: Washington, DC, USA, 2017.

42. ASTM. *D7643*; Standard Practice for Determining the Continuous Grading Temperatures and Continuous Grades for PG Graded Asphalt Binders, American Association of State Highway and Transportation. ASTM: West Conshohocken, PA, USA, 2016.
43. ASTM. *D7175*; Standard Test Method for Determining the Rheological Properties of Asphalt Binder Using a Dynamic Shear Rheometer, American Association of State Highway and Transportation. ASTM: West Conshohocken, PA, USA, 2015.
44. ASTM. *D7405*; Standard Test Method for Multiple Stress Creep and Recovery (MSCR) of Asphalt Binder Using a Dynamic Shear Rheometer, American Association of State Highway and Transportation. ASTM: West Conshohocken, PA, USA, 2020.
45. AFNOR. *NF EN 12697-22*; Bituminous Mixtures. Test Methods: Wheel Tracking, Association Française de Normalisation. AFNOR: Paris, France, 2020.
46. Walubita, L.F.; Faruk, A.N.M.; Zhang, J.; Hu, X.; Lee, S.I. The Hamburg Rutting Test—Effects of HMA Sample Sitting Time and Test Temperature Variation. *Constr. Build. Mater.* **2016**, *108*, 22–28. [CrossRef]
47. Du, Y.; Chen, J.; Han, Z.; Liu, W. A Review on Solutions for Improving Rutting Resistance of Asphalt Pavement and Test Methods. *Constr. Build. Mater.* **2018**, *168*, 893–905. [CrossRef]
48. AASHTO. *M 332*; Standard Specification for Performance-Graded Asphalt Binder Using Multiple Stress Creep Recovery (MSCR) Test, Test Standard Specifications for Transportation Materials and Methods of Sampling and Testing. AASHTO: Washington, DC, USA, 2020.
49. AASHTO. *AASHTO TP 101*; Standard Method of Test for Estimating Fatigue Resistance of Asphalt Binders Using the Linear Amplitude Sweep, Test Standard Specifications for Transportation Materials and Methods of Sampling and Testing. AASHTO: Washington, DC, USA, 2018.
50. Chen, H.; Zhang, Y.; Bahia, H.U. Estimating Asphalt Binder Fatigue at Multiple Temperatures Using a Simplified Pseudo-Strain Energy Analysis Approach in the LAS Test. *Constr. Build. Mater.* **2021**, *266*, 120911. [CrossRef]
51. Chen, H.; Bahia, H.U. Modelling Effects of Aging on Asphalt Binder Fatigue Using Complex Modulus and the LAS Test. *Int. J. Fatigue* **2021**, *146*, 106150. [CrossRef]
52. Kleizienė, R.; Paliukaitė, M.; Vaitkus, A. Effect of Nano SiO_2, TiO_2 and ZnO Modification to Rheological Properties of Neat and Polymer Modified Bitumen. In *Proceedings of the 5th International Symposium on Asphalt Pavements & Environment (APE), ISAP APE 2019, Padua, Italy, 11–13 September 2019*; Lecture Notes in Civil Engineering; Springer: Berlin/Heidelberg, Germany, 2020; Volume 48. [CrossRef]

Disclaimer/Publisher's Note: The statements, opinions and data contained in all publications are solely those of the individual author(s) and contributor(s) and not of MDPI and/or the editor(s). MDPI and/or the editor(s) disclaim responsibility for any injury to people or property resulting from any ideas, methods, instructions or products referred to in the content.